CI&CEQ
Chemical Industry & Chemical Engineering Quarterly

Available on line at
Association of the Chemical Engineers of Serbia *AChE*
www.ache.org.rs/CICEQ

*Chem. Ind. Chem. Eng. Q.* 27 (4) 363–369 (2021) CI&CEQ

HOUARI AMEUR[1]
YOUCEF KAMLA[2]

[1]Department of Technology, University Centre of Naama - Ahmed Salhi, Naama, Algeria
[2]Faculty of Technology, University Hassiba Ben Bouali of Chlef, Algeria

SCIENTIFIC PAPER

UDC 66.063.8:621

# NEWLY SUGGESTED SHAPES OF IMPELLERS FOR STIRRING HIGHLY VISCOUS FLUIDS IN VESSELS

**Article Highlights**

- The agitation of highly viscous fluids in cylindrical tanks is studied numerically
- New shapes of close clearance impellers are suggested
- The performances of the newly designed impellers are compared with those of the classical anchor

**Abstract**

*The power consumption and flow patterns generated in a cylindrical stirred tank are determined. The anchor impeller is used to ensure the agitation of highly viscous fluids. New modifications in the impeller design are introduced to improve the stirring rates. Firstly, the lower corner of the conventional anchor is replaced by an inclined segment to obtain Case No. 1. The number of segments was then increased to reach a closed circular shape (Case No. 2). Further increase in the number of segments was introduced to reach a perfect circular blade (Case No. 3) in the vertical direction. Finally, another circular horizontal blade was added to obtain Case No. 4. From the obtained results, Case No. 4 provided a great improvement in the circulation of fluid particles inside the vessel and generated the widest well-stirred region.*

*Keywords: close clearance impellers, stirred tanks, highly viscous fluids, modified anchor impellers, CFD.*

The stirring in cylindrical tanks is a primary operation to achieve various purposes in different industrial applications, such as the food, paint, polymer, and petroleum industries. In mixing systems, the quality of the final product is strongly related to the flow patterns generated by the stirrer [1-4]. Therefore, details on the hydrodynamics in the whole volume of the stirred tanks are highly needed to be well-known. Further difficulties are encountered during the optimization of processes when the working fluids exhibit high viscosity [5].

The stirred systems containing one or more turbines are generally used for the agitation of low viscous fluids. However, the close clearance impellers are recommended for stirring fluids with high viscosity. In this situation, the stirrer is recommended to be used at low rotational speeds, *i.e.*, under laminar flow conditions [6,7].

For instance, in polymerization processes, the efficiency of mixing should be controlled to avoid some phenomena such as dead poor mixing regions, dead areas, and hot spots [8]. If turbines are employed in the agitation of liquids with high viscosity, the rapid decay of flow velocities may be generated, which yields low blending quality [9].

Various shapes of close clearance stirrers are available in the industry, including the anchor, Maxblend, and helical ribbon. Among these impellers, the anchor has shown satisfactory results. Chhabra and Richardson [10] reported in their research study that the anchor may be utilized for the agitation of Newtonian and non-Newtonian liquids. This type of impellers generates mainly tangential flows, with secondary axial and radial flows at high rotational velocities [11]. In their study on the performance of classical anchor stirrers, Karray *et al.* [12] reported a significant deformation of the anchor arm when operating under

Correspondence: H. Ameur, Department of Technology, University Centre of Naama - Ahmed Salhi, P.O. Box 66, Naama 45000, Algeria.
E-mail: houari_ameur@yahoo.fr
Paper received: 13 October, 2020
Paper revised: 9 January, 2021
Paper accepted: 22 February, 2021

https://doi.org/10.2298/CICEQ201013005A

turbulent flow conditions. They suggested the insertion of an anchor blade to overcome this issue.

Espinosa-Solares *et al.* [13] focused on the influence of wall clearance and bottom clearance on power input. Their findings showed a decrease in power input with the augmentation of the wall and bottom clearance, which is yielded by the change in the hydrodynamics. The experiments conducted by Triveni *et al.* [14] illustrated an increase in the fraction of the well-mixed area from 0.7 to 0.95 with the rise of anchor speeds. This enhancement in the mixing quality was reached for Newtonian and non-Newtonian liquids, however the enhancement was small for highly viscous fluids. With anchor stirrers, Prajapati and Ein-Mozaffari [6] employed the CFD method to estimate the mixing details of viscoplastic fluids. Their optimization study allowed for selecting the values 0.102 and 0.079 as optimum for the stirrer width-to-vessel diameter and the stirrer clearance-to-vessel diameter ratios, respectively. In addition, the anchor with four blades performed better than that with only two blades. Ameur [15] tried to overcome the issue of the deformation of blades by inserting vertical and/or horizontal arms in the blade of the stander anchor. In another paper, Ameur and Ghenaim [16] used Scaba 6SRGT and anchor impellers in a combined configuration to improve the overall efficiency in stirring shear-thinning liquids. Recently, Kamla *et al.* [17] compared the performance of the octagonal, rectangular, and circular design of the blades. The widest well-agitated region was observed as the one with the octagonal shaped blade. However, the circular shaped blade allowed for the lowest power consumption.

In this investigation, new shapes of close clearance stirrers are suggested for the agitation of fluids with high viscosity. The performances of the newly designed impellers are compared with those of the standard anchor. The Newtonian behavior of the working liquid under the laminar flow regime is considered.

## Case study

The geometrical configuration of the agitated system is highlighted in Figure 1. A cylindrical, flat-bottomed, and unbaffled vessel with a diameter $D$ = = 300 mm and height $H/D$ = 1 is used. The glycerol (density $\rho$ = 1262 kg·m$^{-3}$ and viscosity $\mu$ = 1.495 Pa·s) is used as an agitated medium. The vessel is fully filled with the liquid. All necessary details on the other geometrical parameters are given in Table 1. Four newly suggested shapes of close clearance impellers are shown in Figure 1. In Case No. 1, the lower part of the classical anchor impellers has been modified. In Case No. 2, the vertical arms of the blade have been modified to form multiples segments (five segments in each part). Further segments have been introduced in Case No. 2 to form a complete circle, which gives Case No. 3. Finally, Case No. 4 contains

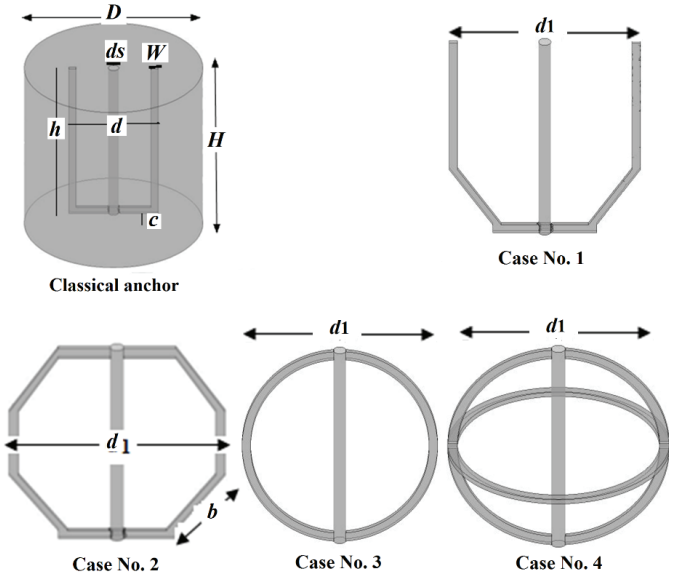


*Figure 1. The different cases under study.*

*Table 1. Values of the geometrcial parameters of the agitation system*

| $H/D$ | $d/D$ | $h/D$ | $c/D$ | $w/D$ | $d_1/D$ | $b/D$ | $d_s/d$ |
|---|---|---|---|---|---|---|---|
| 1 | 0.5 | 0.95 | 0.066 | 0.04 | 0.92 | 0.5 | 0.06 |

two circular shaped blades displayed in horizontal and vertical arrangements. For the classical anchor, the blade diameter is $d$ = 150 mm. For the other cases, the blade diameter is $d_1$ = 276 mm.

### Theoretical tools

The power number ($Np$) is an essential parameter to estimate the efficiency of an agitated tank. It is given as:

$$Np = \frac{P}{\rho N^3 d^5} \quad (1)$$

where $P$ is the power consumption, and $N$ is the impeller rotational velocity. The Reynolds number $Re$ is the ratio between the viscous and inertia forces:

$$Re = \frac{\rho N d^2}{\mu} \quad (2)$$

The dimensionless axial and radial coordinates $Z^*$ and $R^*$ are defined respectively as:

$$R^* = 2R/D \quad (3)$$

$$Z^* = Z/D \quad (4)$$

The dimensionless velocity is defined as:

$$V^* = V/\pi Nd \quad (5)$$

## METHOD

The study is realized via the CFD way by using the computer software (CFX). This software uses the finite volume method to solve the governing equations. The geometry and mesh of the computational domain (Figure 2) were generated with the computer tool Ansys ICEM CFD. The investigations were performed under the following considerations: steady-state, incompressible fluid, three-dimensional and laminar flow conditions. The Rotating Reference Frame (RRF) technique was employed for the modelling of rotating parts. This technique has been selected due to the absence of baffles [18-23]. To achieve the velocity-pressure coupling, a pressure-correction method of the semi-implicit method for pressure-linked equations-consistent type (SIMPLEC) was used. Due to its high precision, the second-order central scheme with the finite volume method was utilized. The grids were refined near the impeller and vessel walls to capture the flow boundary details. To determine the optimal grid size for the computational domain, the mesh density was increased by about 2. Mesh tests were carried out by checking that the additional grids did not change the velocity magnitude in regions with high gradients by more than 2.5% (Table 2). From these results, the mesh M2 with a global number of cells of about 821,584 was selected as optimal.

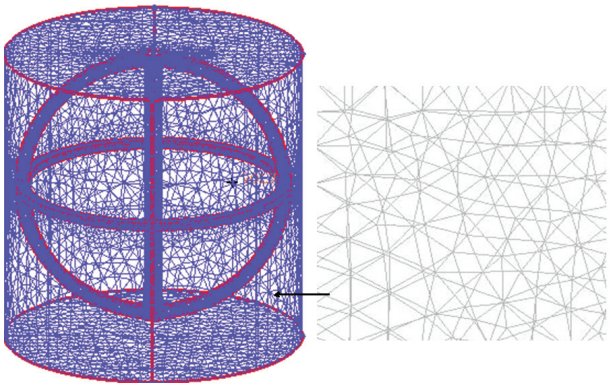

*Figure 2. Meshing of the computational domain.*

*Table 2. Details on mesh tests for Case No. 1 at Re = 50*

| Parameter | M1 | M2 | M3 |
|---|---|---|---|
| Number of cells | 401,145 | 821,584 | 1,520,548 |
| $Np$ | 1.9411 | 1.9622 | 1.9671 |
| Time required, s | 3,520 | 7,215 | 14,415 |

With a machine (Intel® i7 processor with 8 Gb RAM) and for a residual target $10^{-7}$, the convergence was achieved after about 1700-1800 iterations, which corresponds to about 2-3 h of CPU time.

### Validation

To check the good and appropriate settings of boundary conditions, as well as the selected computational grid, some computed findings were compared against the available experimental data. Figure 3a shows our results of power number that are obtained numerically and those obtained experimentally by Prajapati and Ein-Mozaffari [6]. While Figure 3b illustrates the variation of tangential velocity *vs.* vessel radius ($R^*$) at $Re$ = 14. In Figure 3b, the validation is made against the experimental data of Anne-Archard *et al.* [24]. As it may be observed, the validation in both figures reveals a satisfactory agreement.

## RESULTS AND DISCUSSION

### Flow fields

In this section, the flow fields and velocities are highlighted at various positions in the tank and under various plots. At the mid-height of the tank ($Z^*$ = 0.5) and for the angular position $\theta$ = 0°, the distribution of the dimensionless tangential velocity ($V_\theta^*$) along with the tank radius ($R^*$) is plotted in Figure 4. The values of $V_\theta^*$ are given for the five geometrical cases under inspection. For all the computations, the line passing

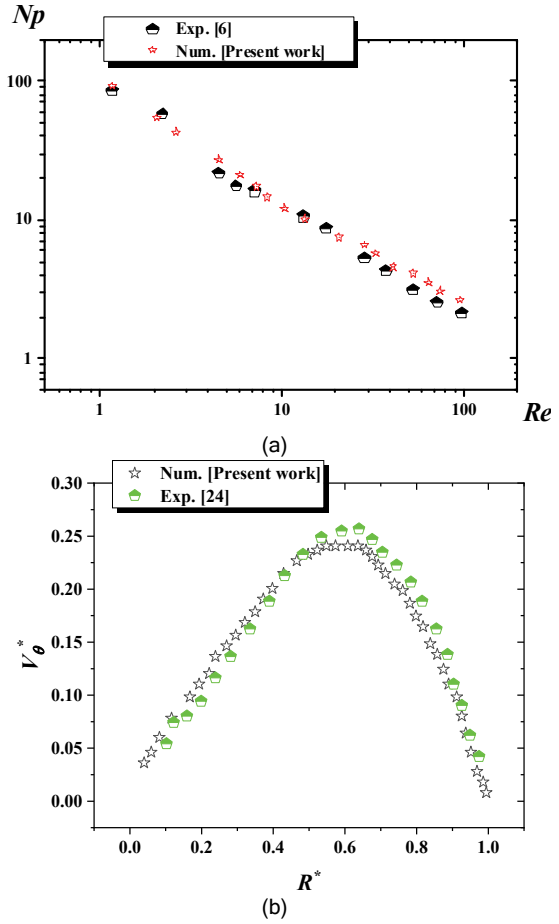


*Figure 3. Validation of the computed results: a) power number (Np) vs. Reynolds number (Re); b) variation of the tangential velocity at Re = 14.*

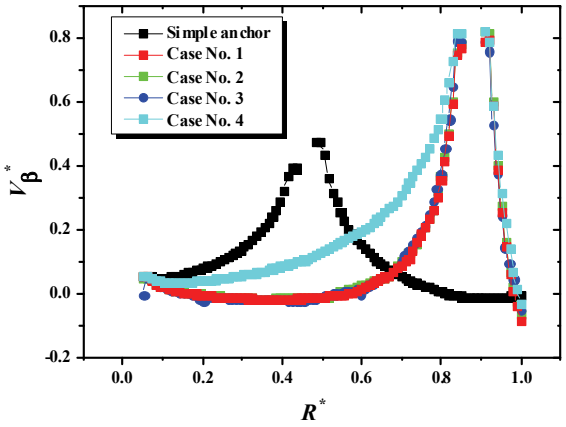


*Figure 4. Tangential velocity for Re = 50, $Z^* = 0.5$, and $\theta = 0°$.*

through the blade of the classical anchor impeller is taken as a reference for the angular coordinate.

As shown in this figure, $V_\theta^*$ augments gradually from the agitator shaft until reaching the highest values at the blade tip, and it decreases again until becoming negligible at the tank wall. The comparison between the different suggested shapes indicates that the maximum amount of $V_\theta^*$ is reached at the blade tip, whatever the shape of the blade. In addition, the lowest amount of the velocity is observed for the classical anchor because $d < d_1$.

The results of $V_\theta^*$ at the angular position $\theta = 90°$ are illustrated in Figure 5. At this location, the velocity changes according to parabolic profiles. From the different cases, the impeller that contains two circular blades (*i.e.*, Case No. 4) yielded the most powerful tangential flows, followed by the impeller that contains only one circular blade. A slight difference between the classical anchor, Cases No. 1-3 is observed in terms of velocity intensity. However, the difference between the mentioned cases and Case No. 4 is very large, which is due to the existence of the second circular blade.

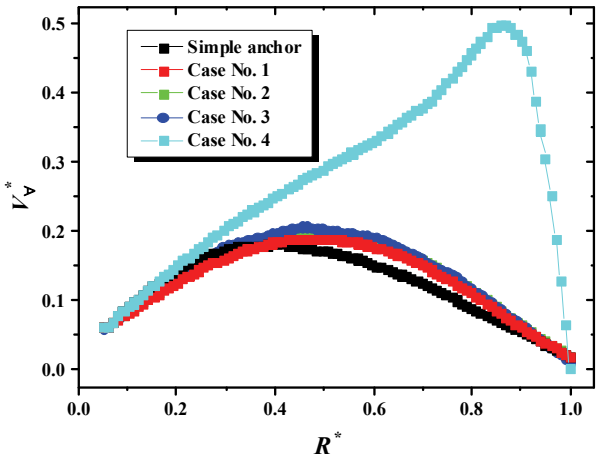


*Figure 5. Tangential velocity for Re = 50, $Z^* = 0.5$, and $\theta = 90°$.*

Further insight into the hydrodynamics generated by the different stirrers is provided by the results of Figures 6 and 7. The streamlines induced by the different cases are presented in Figure 6 at the mid-height of the tank for the angular position $\theta = 90°$. The classical anchor generates tangential flows in the whole vessel volume. The toroidal flow observed in this figure for the classical anchor is due to the wall effect (vessel and impeller shaft). This toroidal flow is formed in the lower part of the vessel for Cases No. 1 and 2 due to the modifications introduced in the blade. The flow is almost uniform at the lower part of the vessel for all cases, except Case No. 4, where the presence of the second horizontal blade destroyed this uniformity of the flow and generated another toroidal flow. Furthermore, the size of the toroidal structure of the flow is the highest for Case No. 4.

The results of the velocity contours at the mid-height of the tank are illustrated in Figure 7. It seems that the classical anchor has the lowest size of the

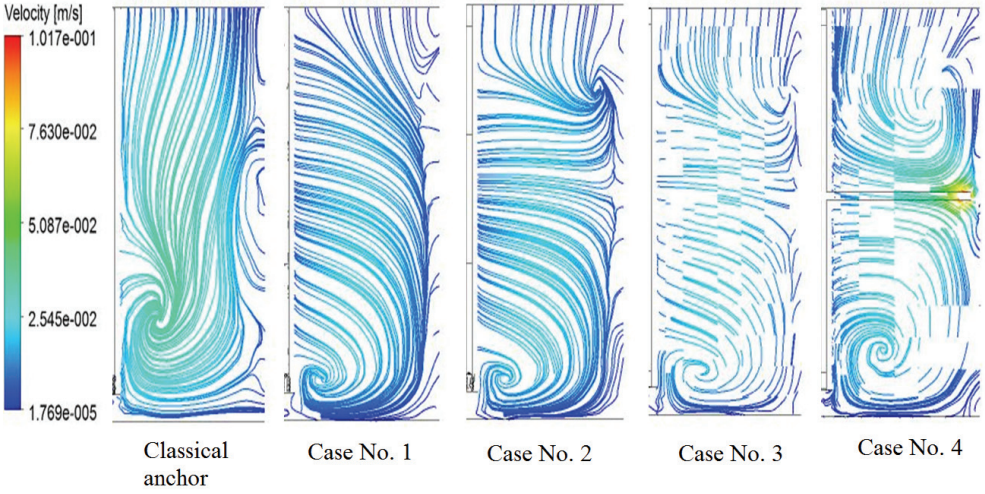


*Figure 6. Streamlines for Re = 50 and θ = 90°.*

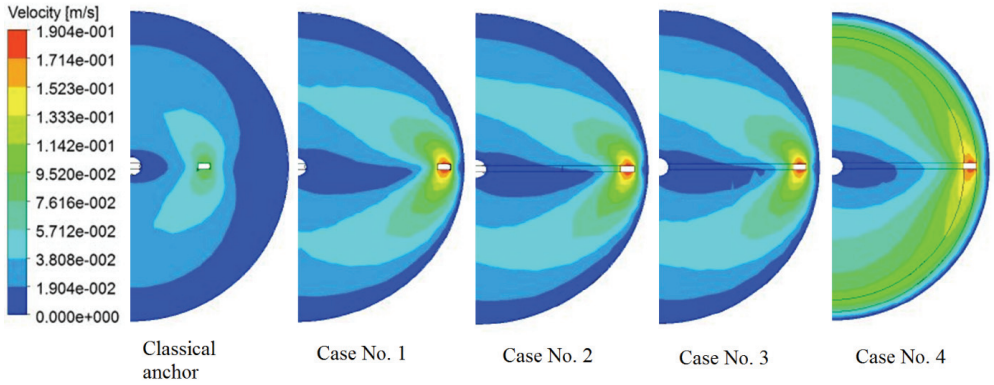


*Figure 7. Well-agitated region at Re = 50, $Z^* = 0.5$.*

well-stirred region. The introduction of an inclined arm at the lower part of the conventional anchor allowed a little increase in the size of the agitated area. However, a small enhancement has been obtained with Case No. 2, which remained almost the same with Case No. 3. The insertion of another horizontal circular blade (Case No. 4) has overcome the issue of the poor agitated region at some angular positions and it has given a satisfactory distribution of flow velocities. Finally, and in terms of uniformity of the flows, the studied impellers may be classified as follows: Case No. 4, 3/2, 1, and then the classical anchor.

## Power consumption

The power consumption is another issue to be verified in stirred tanks. The results of the power number (*Np*) for the different geometrical configurations are given in Figure 8 for various Reynolds numbers. A continuous decrease in *Np* values is reached with the increased impeller rotational speeds (*Re*). This decrease is highly significant in the deep laminar regime.

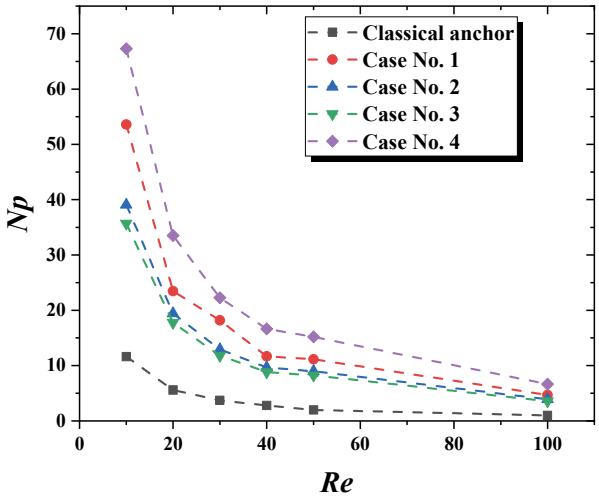


*Figure 8. Power number vs. Reynolds number.*

The lowest values of *Np* were reached with the classical anchor due its small blade diameter. The comparison between the classical anchor and Case No. 1 showed an increase in *Np* values by about four times due to the increased blade diameter. Moving

from Case No. 1 to Case No. 2, the power number was increased by about 20%. However, moving from Case No. 2 to Case No. 3, only a slight decrease in *Np* was observed. Adding another circular horizontal blade has yielded an increase in *Np* by about 50% in comparison between Cases No. 3 and 4. For example, at *Re* = 50, the values of the power number are 1.96, 11.13, 8.97, 8.23, and 15.19 for the classical anchor, Cases No. 1–4, respectively.

## CONCLUSION

Some modifications in the classical anchor impeller have been suggested to improve the hydrodynamic characteristics in cylindrical vessels. In each part of the blade of the conventional anchor, the lower corner was replaced by an inclined segment to obtain the so referenced Case No. 1 in this study. Then, the number of these segments were increased to form a closed shape (Case No. 2). Further segments were added to obtain a perfect circular blade (Case No. 3) in a vertical position. Finally, another horizontal circular blade was added to give Case No. 4.

From the obtained results, the suggested Case No. 4 allowed a significant enhancement in the movement of the fluid particles in the entire volume of the stirred vessel. This case has given a satisfactory distribution of flow velocities and it has generated the widest well-stirred area. In terms of less power consumption, the newly suggested shapes of impeller may be classified as follows: Cases No. 3, 2, 1 and 4. For industrial applications, further studies on the newly proposed design are needed for other kinds of fluids and operating conditions to allow the good choice of the most efficient impeller.

### Nomenclature

$b$ - Length of the blade segment, m
$c$ - Impeller off-bottomed clearance, m
$D$ - Tank diameter, m
$d$, $d_1$ - Agitator diameter, m
$d_s$ - Diameter shaft, m
$h$ - Blade height, m
$H$ - Tank height, m
$N$ - Agitator rotational speed, $s^{-1}$
$Np$ - Power number, dimensionless
$P$ - Power, W
$R$ - Radial coordinate, m
$R^*$ - Dimensionless radial coordinate, $R^* = 2R/D$
$Re$ - Reynolds number, dimensionless
$V_z$ - Axial velocity, $m \cdot s^{-1}$
$V_\theta$ - Tangential velocity, $m \cdot s^{-1}$
$W$ - Thickness of the blade arm, m
$Z$ - Axial coordinate, m
$Z^*$ - Dimensionless axial coordinate, $Z^* = Z/D$
$\rho$ - Fluid density, $kg \cdot m^{-3}$
$\mu$ - Viscosity, Pa·s

## REFERENCES


[1] S. Deshpande, K. Kar, J. Walker, J. Pressler, W. Su, Chem. Eng. Sci. 168 (2017) 495-506
[2] G. Janiga, Chem. Eng. Sci. 201 (2019) 132-144
[3] H. Ameur, Chem. Eng. Proc. Process Intensif. 154 (2020) 108009
[4] M. Foukrach, H. Ameur, Chem. Ind. Chem. Eng. Q. 26 (2020) 259-266
[5] H. Ameur, Energy 93 (2015) 1980-1988
[6] P. Prajapati, F. Ein-Mozaffari, Chem. Eng. Technol. 32 (2009) 1211-1218
[7] H. Ameur, ChemistrySelect 2 (2017) 11492-11496
[8] B. Triveni, B. Vishwanadham, T. Madhavi, S. Venkateshwar, Chem. Eng. Res. Des. 88 (2010) 809-818
[9] S. Woziwodzki, L. Broniarz-Press, M. Ochowiak, Chem. Eng. Technol. 33 (2010) 1099-1106
[10] R.P. Chhabra, J.F. Richardson, Non-Newtonian flow in the process industries: fundamentals and engineering applications, Butterworth-Heinemann, Oxford, 1999
[11] M. Ohta, M. Kuriyama, K. Arai, S. Saito, J. Chem. Eng. Japan 18 (1985) 81-84
[12] S. Karray, Z. Driss, H. Kchaou, M. Abid, Eng. Appl. Comp. Fluid Mech. 5 (2011) 315-328
[13] T. Espinosa-Solares, E.B.-D.L. Fuente, F. Thibault, P. Tanguy, Chem. Eng. Commun. 157 (1997) 65-71
[14] B. Triveni, B. Vishwanadham, S. Venkateshwar, Heat Mass Transfer 44 (2008) 1281-1288
[15] H. Ameur, J. Hydrodyn. 28 (2016) 669-675
[16] H. Ameur, A. Ghenaim, ChemistrySelect 3 (2018) 7472--7477
[17] Y. Kamla, H. Ameur, A. Karas, M.I. Arab, Chem. Pap. 74 (2020) 779-785
[18] R. Alcamo, G. Micale, F. Grisafi, A. Brucato, M. Ciofalo, Chem. Eng. Sci. 60 (2005) 2303-2316
[19] A. Khapre, B. Munshi, J. Taiwan Inst. Chem. Eng. 56 (2015) 16-27
[20] A. Hadjeb, M. Bouzit, Y. Kamla, H. Ameur, Polish J. Chem. Technol. 19 (2017) 83-91
[21] H. Ameur, Chin. J. Chem. Eng. 24 (2016) 572-580
[22] H. Ameur, Int. J. Chem. React. Eng. 14 (2016) 1025-1033
[23] H. Ameur, J. Food Eng. 233 (2018) 117-125
[24] D. Anne-Archard, H. C. Boisson, M. Marouche, in Proceedings of 18ème Congrès Français de Mécanique, Grenoble, France, 2007, pp. 27-31.

**HOUARI AMEUR[1]**
**YOUCEF KAMLA[2]**

**[1]Department of Technology, University Centre of Naama - Ahmed Salhi, Naama, Algeria**
**[2]Faculty of Technology, University Hassiba Ben Bouali of Chlef, Algeria**

NAUČNI RAD

# NOVI TIPOVI MEŠALICA ZA MEŠANJE VISKOZNIH TEČNOSTI U SUDOVIMA

*Određeni su snaga mešanja i obrasci strujanja u cilindričnom sudu sa mešalicom. Sidrasta mešalica je korišćena za mešanje jako viskoznih tečnosti. Uvedene su nove modifikacije u dizajnu mešalice da bi se poboljšale brzine mešanja. Prvo, donji ugao konvencionalnog sidra je zamenjen kosim segmentom (tip 1). Broj segmenata je zatim povećan da bi se postigao zatvoreni kružni oblik (tip 2). Dalje povećanje broja segmenata je uvedeno da bi se postiglo savršeno kružno sečivo (tip 3) u vertikalnom pravcu. Konačno, dodato je još jedno kružno horizontalno sečivo (tip 4). Tip 4 je značajno poboljšao cirkulaciju tečnosti unutar suda i stvorio najširu dobro izmešanu oblast.*

*Ključne reči: Sidraste mešalice; suds a mešanjem; jako viskozne tečnosti; modifikovane sidraste mešalice; CFD.*